

Electronic Supplementary Information (ESI)

Structure and magnetic properties of two $\{\text{Co}^{\text{III}}\text{M}^{\text{II}}\}$ cyanide bridged chains

Maria-Gabriela Alexandru, Diana Visinescu, Sergiu Shova, Abdeslem Bentama, Francesc Lloret, Joan Cano and Miguel Julve

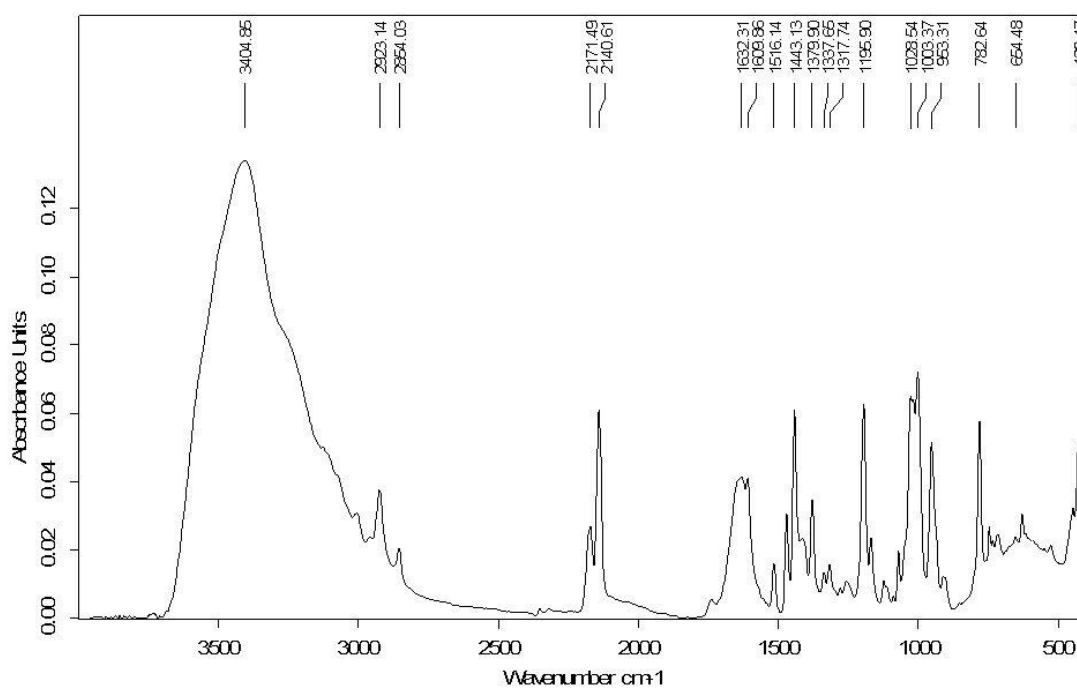


Figure S1. FTIR spectrum for 1.

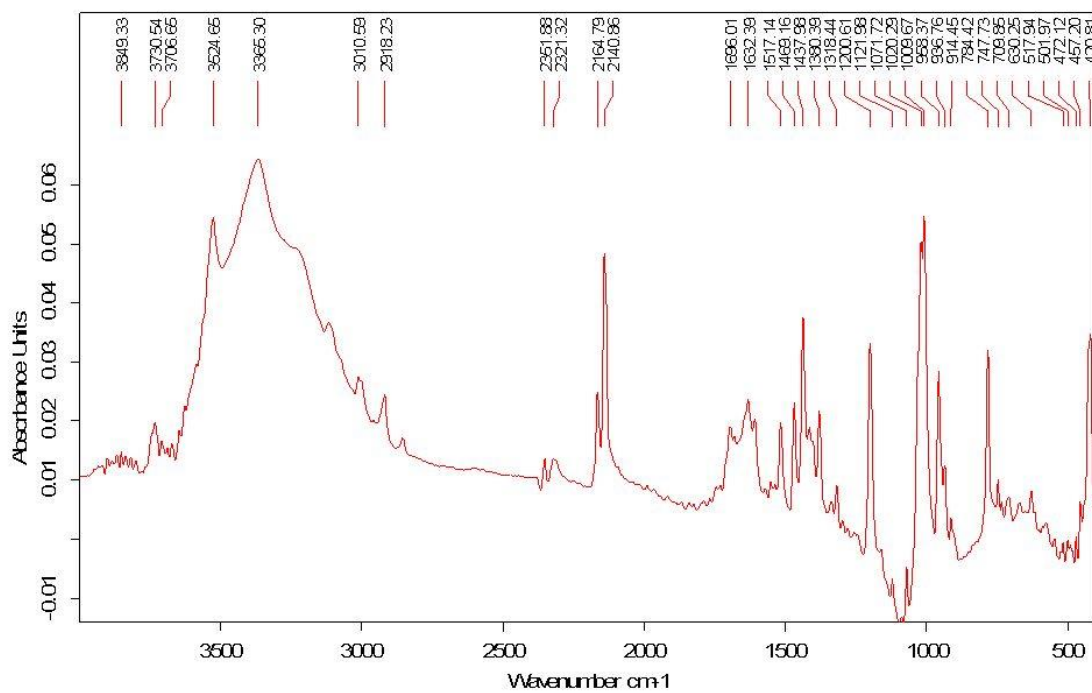


Figure S2. FTIR spectrum for **2**.

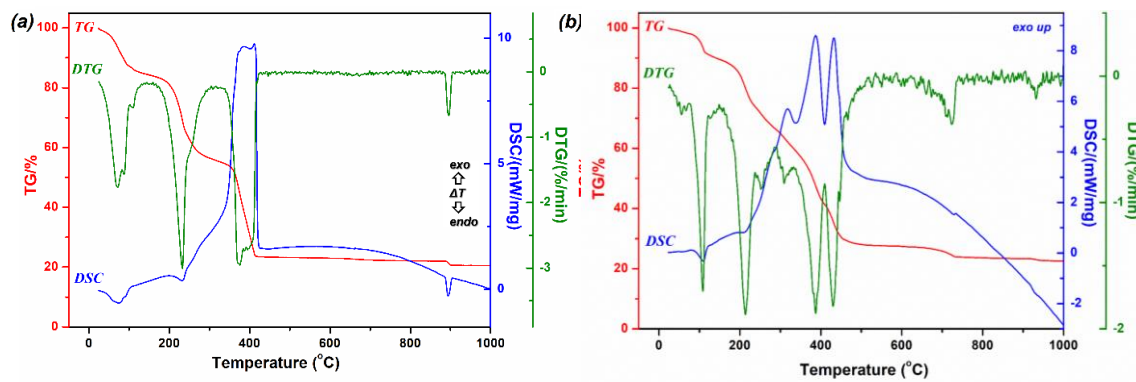


Figure S3. Thermal curves (TG, DTG, and DSC) of **1** (a) and **2** (b) in the 25–1000 °C temperature range.

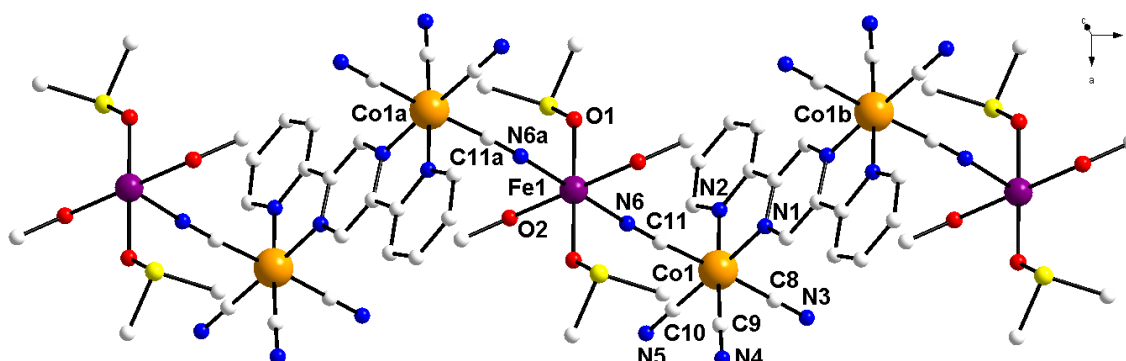


Figure S4. View of a fragment the chain structure of **2**, along with the atom labelling.

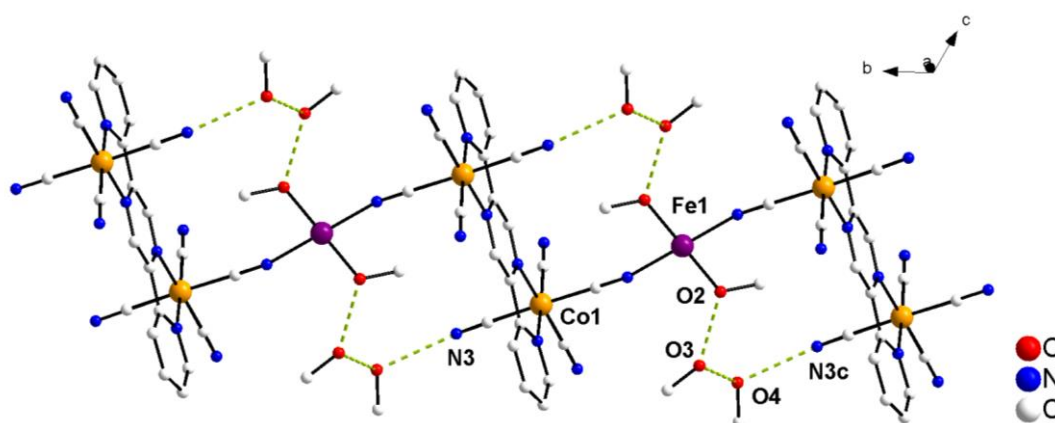


Figure S5. A view of the hydrogen bonding pattern in **2**. The DMSO molecules were omitted for clarity [Symmetry code: (c) = x, -1+y, z].

Table S1. Results of the SHAPE analysis of the $\{Co^{III}C_4N_2\}$ and $\{M^{II}N_2O_4\}$ chromophores from the $\{Co^{III}(DPP)_{1/2}(CN)_4\}^-$ (**1** and **2**) and $\{M^{II}(CN)_2(H_2O)_2(DMSO)_2\}$ fragments [$M = Co^{II}$ (**1**) and Fe^{II} (**2**)].

$[Co^{III}C_4N_2]$	HP-6	PPY-6 ^a	OC-6 ^a	TPR-6 ^a	JPPY-5 ^a
1	31.162	28.446	0.212	15.716	31.709
2	31.029	28.283	0.202	15.743	31.588
$[M^{II}N_2O_4]$					
1 (M = Co)	31.623	29.481	0.093	16.046	32.835
2 (M = Fe)	31.460	29.244	0.065	16.442	32.513

^aHP-6, D_{6h} , Hexagon; PPY-6, C_{5v} Pentagonal pyramid; OC-6, O_h Octahedron; TPR-6, D_{3h} Trigonal prism; JPPY-5, C_{5v} Johnson pentagonal pyramid (J2).

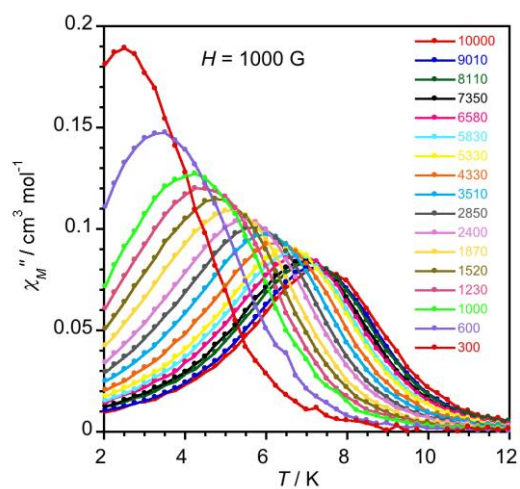


Figure S6. Thermal dependence of χ_M'' for **1** under an applied static field of $H_{dc} = 1000$ G with a ± 5 G oscillating field at frequencies in the range 0.3-10 kHz.

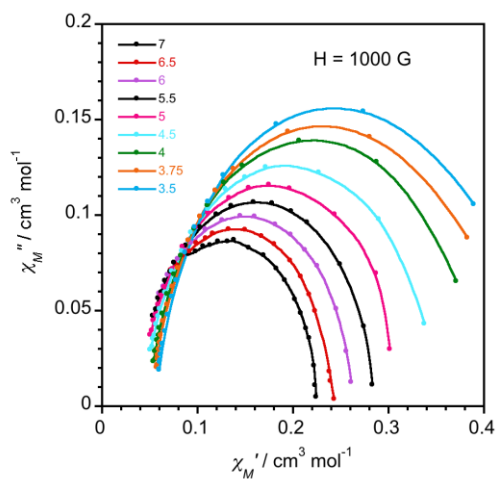


Figure S7. Cole-Cole plots in the temperature range 3.5-7.0 K for **1** under an applied static field $H_{dc} = 1000$ G. The solid lines are the best-fit curves.

Table S2. Energy of the calculated quartet (Q_i) and doublet (D_i) excited states and their contributions to the D and E values for **1** obtained from CASSCF/NEVPT2 calculations. D_{SS} is the spin-spin contribution to axial zfs parameter, and D_Q and D_D are the sum of spin-orbit contributions coming from quartet and doublet excited states

State	Energy ^a	S	D^a	E^a	State	Energy ^a	S	D^a	E^a
D_{SS}		4	+0.000	+0.000	D_5	20091.0	2	-1.217	-1.194
D_Q		4	+56.696	+12.251	D_6	20133.8	2	-0.580	+0.577
D_D		2	+6.472	-1.558	D_7	20769.4	2	-0.746	+0.670
Q_1	847.0	4	+32.999	+33.576	D_8	20998.3	2	-0.036	-0.055
Q_2	1343.4	4	+18.949	-18.953	D_9	23166.6	2	+3.869	-0.001
Q_3	7894.0	4	-1.684	+3.725	D_{10}	23514.6	2	-0.007	+0.005
Q_4	8262.3	4	+5.780	-5.951	D_{11}	23722.3	2	-0.005	+0.000
Q_5	10058.1	4	+0.371	-0.144	D_{12}	25873.8	2	-0.028	-0.032
Q_6	17976.3	4	+0.006	+0.002	D_{13}	29237.8	2	-0.397	+0.095
Q_7	22258.8	4	+0.079	-0.074	D_{14}	29261.4	2	-0.357	-0.031
Q_8	22721.1	4	+0.019	-0.015	D_{15}	30383.8	2	+0.005	-0.059
Q_9	23477.5	4	+0.087	+0.085	D_{16}	30500.1	2	+0.021	-0.015
D_1	11514.6	2	+1.101	+0.123	D_{17}	30773.6	2	-0.018	+0.015
D_2	13216.4	2	+4.063	-1.426	D_{18}	31985.3	2	-0.029	+0.029
D_3	18488.5	2	-0.055	+0.039	D_{19}	32301.0	2	+1.018	-0.209
D_4	19630.6	2	-0.007	+0.003	D_{20}	33135.2	2	-0.122	-0.092

^aValues in cm^{-1} .

Table S3. Energy of the calculated quintet (Q_i) and triplet (D_i) excited states and their contributions to the D and E values for **2** obtained from CASSCF/NEVPT2 calculations. D_{SS} is the spin-spin contribution to axial zfs parameter, and D_Q and D_D are the sum of spin-orbit contributions coming from quartet and doublet excited states

State	Energy ^a	S	D^a	E^a	State	Energy ^a	S	D^a	E^a
D_{SS}		4	+0.000	+0.000	D_{13}	26239.2	3	-0.006	-0.014
D_Q		4	+5.726	+1.028	D_{14}	26647.7	3	+0.024	-0.005
D_D		2	+1.284	+1.308	D_{15}	26658.5	3	+0.612	+0.044
Q_1	1605.9	5	+2.982	-1.782	D_{16}	26827.9	3	+0.077	+0.006
Q_2	1972.8	5	+1.963	+1.469	D_{17}	27904.5	3	-0.092	+0.196
Q_3	9725.9	5	+1.229	+1.314	D_{18}	30479.5	3	-0.203	+0.139
Q_4	11740.8	5	-0.448	+0.027	D_{19}	30904.0	3	-0.141	-0.155
D_1	14947.9	3	-0.559	+0.875	D_{20}	30987.1	3	+0.920	-0.065
D_2	16125.9	3	+0.080	-0.037	D_{21}	31091.8	3	-0.182	+0.063
D_3	16341.5	3	+1.138	+0.134	D_{22}	33095.9	3	-0.053	+0.079
D_4	19556.0	3	-0.190	-0.140	D_{23}	33417.9	3	-0.009	-0.002
D_5	20758.5	3	-0.025	-0.024	D_{24}	33732.8	3	-0.004	-0.003
D_6	21638.4	3	-0.103	+0.069	D_{25}	34738.3	3	+0.179	+0.020
D_7	23598.3	3	+0.003	-0.000	D_{26}	35337.2	3	+0.019	+0.000
D_8	23835.8	3	+0.116	+0.018	D_{27}	35857.0	3	-0.007	-0.005
D_9	24909.6	3	-0.059	+0.119	D_{28}	36760.4	3	-0.153	-0.065
D_{10}	25655.6	3	+0.003	+0.000	D_{29}	37082.9	3	-0.071	+0.046
D_{11}	26083.1	3	+0.018	-0.002	D_{30}	37801.1	3	-0.055	+0.022
D_{12}	26195.1	3	+0.007	-0.005					

^aValues in cm^{-1} .

Table S4. Parameters of the fit of the ac magnetic susceptibility data of **1** through the Debye model

H_{dc} / G	T / K	$\chi_t / \text{cm}^3 \text{mol}^{-1}$	$\chi_s / \text{cm}^3 \text{mol}^{-1}$	α
1000	3.50	0.442	0.0552	0.1100
	3.75	0.423	0.0510	0.1220
	4.00	0.397	0.0476	0.1230
	4.50	0.353	0.0422	0.1210
	5.00	0.312	0.0397	0.0937
	5.50	0.286	0.0369	0.0901
	6.00	0.264	0.0354	0.0801
	6.50	0.240	0.0349	0.0790
2500	3.50	0.415	0.0152	0.1160
	3.75	0.402	0.0131	0.1330
	4.00	0.372	0.0130	0.1220
	4.50	0.352	0.0122	0.1540
	5.00	0.312	0.0119	0.1350
	5.50	0.276	0.0117	0.1260
	6.00	0.262	0.0114	0.0972
	6.50	0.242	0.0110	0.0868

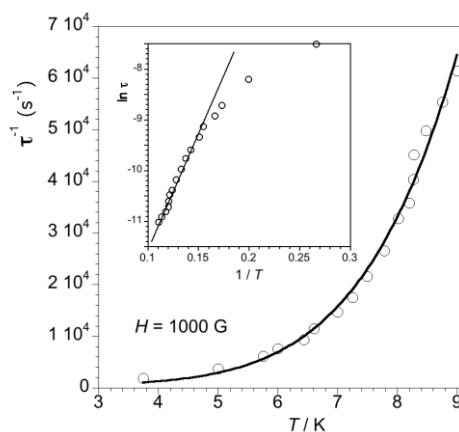


Figure S8. Temperature dependence of τ^{-1} (o) for **1** under $H_{dc} = 1000 \text{ G}$ showing the best fit (solid line) to the combination of a direct and one Raman approach. The inset is the Arrhenius plot (o) showing the best-fit (solid line) to one Orbach process.